

NANO EXPRESS

Open Access

Manipulation of domain wall dynamics in amorphous microwires through the magnetoelastic anisotropy

Arcady Zhukov^{1,2*}, Juan Maria Blanco³, Mihail Ipatov¹, Alexander Chizhik¹ and Valentina Zhukova¹**Abstract**

We studied the effect of magnetoelastic anisotropy on domain wall (DW) dynamics and remagnetization process of magnetically bistable Fe-Co-rich microwires with metallic nucleus diameters (from 1.4 to 22 μm). We manipulated the magnetoelastic anisotropy applying the tensile stresses and changing the magnetostriction constant and strength of the internal stresses. Microwires of the same composition of metallic nucleus but with different geometries exhibit different magnetic field dependence of DW velocity with different slopes. Application of stresses resulted in decrease of the DW velocity, v , and DW mobility, S . Quite fast DW propagation (v until 2,500 m/s at H about 30 A/m) has been observed in low magnetostrictive magnetically bistable $\text{Co}_{56}\text{Fe}_8\text{Ni}_{10}\text{Si}_{10}\text{B}_{16}$ microwires. Consequently, we observed certain correlation between the magnetoelastic energy and DW dynamics in microwires: decreasing the magnetoelastic energy, K_{me} , DW velocity increases.

Background

Recent growing interest on domain wall (DW) propagation in thin magnetic wires with submicrometric and micrometric diameter is related with proposals for prospective logic and memory devices [1,2]. In these devices, information can be encoded in the magnetic states of domains in lithographically patterned nanowires [2]. DW motion along the wires allows manipulation of the stored information. The speed at which a DW can travel in a wire has an impact on the viability of many proposed technological applications in sensing, storage, and logic operation [2]. When a DW is driven by a magnetic field, H , parallel to the wire axis, the maximum wall speed is found to be a function of magnetic field and the wire dimensions [1,3-7]. This propagation can be driven by magnetic fields [8] reaching velocities up to 1,000 m/s or by spin-polarized electric currents in the nanowires [9]. In fact, it is essentially important not only fast domain wall propagation itself but also controlling of domain wall pinning in thin magnetic wires. Several methods of controlling domain walls in nanowires

have been reported. For example, domain walls can be introduced to nanowires at low fields by injection from a large, magnetically soft region connected to a wire end using a lithographically fabricated current carrying wire to provide local field or heating [1,2]. Domain walls have been pinned at artificially created defects in thin wires elsewhere [1,2].

Last few years studies of current- and magnetic field-driven domain wall propagation in different families of thin magnetic wires (planar and cylindrical) attracted considerable attention [1-3]. Considerable attention has been paid to achieve controllable and fast domain wall propagation in thin magnetic wires (planar and cylindrical) taking into account the possibility to use it for high-density data storage devices (magnetic random memory devices, logic devices) [1].

It is worth mentioning that extremely fast DW propagation of single domain wall at relatively low magnetic field has been reported for cylindrical glass-coated amorphous microwires with positive magnetostriction constant with typical diameters of ferromagnetic nucleus about 10 to 20 μm [3,4].

Glass-coated ferromagnetic wires exhibit unusual and interesting magnetic properties such as magnetic bistability and giant magneto-impedance effect [3,5,6]. Magnetic

* Correspondence: arkadi.joukov@ehu.es¹Department of Material Physics, Chemistry Faculty, Universidad del País Vasco/Euskal Herriko Unibertsitatea (UPV/EHU), P.O. Box 1072, San Sebastián 20080, Spain²IKERBASQUE, Basque Foundation for Science, Bilbao 48011, Spain

Full list of author information is available at the end of the article

bistability, observed previously in few amorphous materials, is related with single and large Barkhausen jump [3,5,7]. Such behavior observed in different wire families has been interpreted as the magnetization reversal in a single large axially magnetized domain [3,8]. From the point of view of studies of DW dynamics, amorphous glass-coated microwires with positive magnetostriction constant are unique materials allowing us to study the magnetization dynamics of a single DW in a cylindrical micrometric wire. It is commonly assumed that their domain structure is determined by the stress distribution during rapid solidification fabrication process and consists of single large axial domain with magnetization oriented axially and the external domain structure with radial magnetization at the surface [3,5,8]. The magnetization process in axial direction runs through the propagation of the single head-to-head DW. It is worth mentioning that the micromagnetic origin of rapidly moving head-to-head DW in microwires is still unclear, although there are evidences that this DW is relatively thick and has complex structure [9].

At the same time, it is commonly assumed that the preparation of glass-coated microwires involving simultaneous solidification of composite microwire consisting of ferromagnetic metallic nucleus inside the glass coating introduces considerable residual stresses inside the ferromagnetic metallic nucleus [5,10]. The strength of internal stresses is determined by the thickness of glass coating and metallic nucleus diameter. This additional magnetoelastic anisotropy affects soft magnetic properties of glass-coated microwires. Consequently, one can expect that DW dynamics should be considerably affected by this magnetoelastic anisotropy. However, until now, little attention has been paid to studies of the influence of magnetoelastic anisotropy on DW dynamics in microwires [5,11].

Therefore, the purpose of this paper is to reveal the effect of magnetoelastic anisotropy on DW propagation in amorphous magnetically bistable microwires.

Methods

We prepared a number of amorphous Fe-Co-based glass-coated microwires with different magnetostriction constants using Taylor-Ulitovsky method, as described in [3-5,8,11]. Studied microwires of $\text{Co}_{56}\text{Fe}_8\text{Ni}_{10}\text{Si}_{10}\text{B}_{16}$, $\text{Co}_{41.7}\text{Fe}_{36.4}\text{Si}_{10.1}\text{B}_{11.8}$, $\text{Fe}_{55}\text{Co}_{23}\text{B}_{11.8}\text{Si}_{10.2}$, $\text{Fe}_{16}\text{Co}_{60}\text{Si}_{11}\text{B}_{13}$, $\text{Fe}_{72.75}\text{Co}_{2.25}\text{B}_{15}\text{Si}_{10}$, and $\text{Fe}_{70}\text{B}_{15}\text{Si}_{10}\text{C}_5$ compositions of ferromagnetic nucleus have positive magnetostriction constant and diameters of metallic nucleus from 1.2 to 22 μm . It is worth mentioning that the magnetostriction constant, λ_s , in system $(\text{Co}_x\text{Fe}_{1-x})_{75}\text{Si}_{15}\text{B}_{10}$ changes with x from -5×10^{-6} at $x = 1$ to $\lambda_s \approx 35 \times 10^{-6}$ at $x \approx 0.2$. Therefore, producing microwires with various Fe-Co-rich compositions, we changed the magnetostriction constant from $\lambda_s \approx 35 \times 10^{-6}$ for Fe-rich compositions ($\text{Fe}_{72.75}\text{Co}_{2.25}\text{B}_{15}\text{Si}_{10}$ and $\text{Fe}_{70}\text{B}_{15}\text{Si}_{10}\text{C}_5$) to $\lambda_s \approx 10^{-7}$ for $\text{Co}_{56}\text{Fe}_8\text{Ni}_{10}\text{Si}_{10}\text{B}_{16}$ microwire (see sample details and properties in Table 1).

Within each composition of metallic nucleus, we also produced microwires with different ratios of metallic nucleus diameter and total diameter, D , i.e., with different ratios $\rho = d/D$. This allowed us to control residual stresses since the strength of internal stresses is determined by ρ ratio [5,8]. We used simple measurement method based on the classical Sixtus-Tonks-like experiments [13] and measured DW dynamics under tensile applied stresses.

It is worth mentioning that the magnetoelastic energy, K_{me} , is given by:

$$K_{me} \approx 3/2 \lambda_s \sigma \quad (1)$$

where $\sigma = \sigma_i + \sigma_a$ is the total stress; σ_i , the internal stresses; σ_a , the applied stresses; and λ_s , the magnetostriction constant [5,8,14,15].

In this way, we studied the effect of magnetoelastic contribution on DW dynamics controlling the magnetostriction constant, applied, and/or residual stresses.

Table 1 Sample compositions, geometrical features, and properties

Sample composition	Sample number	Sample geometry: ρ ratio, metallic nucleus diameter, d , and total diameter, D	Magnetostriction constant ^a
$\text{Co}_{56}\text{Fe}_8\text{Ni}_{10}\text{Si}_{10}\text{B}_{16}$	1	$\rho \approx 0.45$, $d \approx 13.2 \mu\text{m}$, $D \approx 29.6 \mu\text{m}$	10^{-7}
$\text{Co}_{41.7}\text{Fe}_{36.4}\text{Si}_{10.1}\text{B}_{11.8}$	2A2B	$\rho = 0.39$, $d \approx 13.6 \mu\text{m}$, $D \approx 34 \mu\text{m}$; $\rho \approx 0.55$, $d \approx 13.6 \mu\text{m}$, $D \approx 24.6 \mu\text{m}$	25×10^{-6}
$\text{Fe}_{55}\text{Co}_{23}\text{B}_{11.8}\text{Si}_{10.2}$	3A3B	$\rho \approx 0.44$, $d \approx 13.2 \mu\text{m}$, $D = 29.6 \mu\text{m}$; $\rho \approx 0.55$, $d \approx 12.6 \mu\text{m}$, $D = 22.8 \mu\text{m}$	30×10^{-6}
$\text{Fe}_{16}\text{Co}_{60}\text{Si}_{11}\text{B}_{13}$	4	$\rho \approx 0.39$, $d \approx 13.6 \mu\text{m}$, $D \approx 34.5 \mu\text{m}$	15×10^{-6}
$\text{Fe}_{72.75}\text{Co}_{2.25}\text{B}_{15}\text{Si}_{10}$	5A5B	$\rho \approx 0.14$, $d \approx 1.4 \mu\text{m}$, $D \approx 10 \mu\text{m}$; $\rho \approx 0.31$, $d \approx 2.8 \mu\text{m}$, $D \approx 9 \mu\text{m}$	35×10^{-6}
$\text{Fe}_{70}\text{B}_{15}\text{Si}_{10}\text{C}_5$	6A6B6C 6D6E	$\rho \approx 0.67$, $d \approx 14.6 \mu\text{m}$, $D \approx 21.8 \mu\text{m}$; $\rho \approx 0.63$, $d \approx 15 \mu\text{m}$, $D \approx 23.8 \mu\text{m}$; $\rho \approx 0.48$, $d \approx 10.8 \mu\text{m}$, $D \approx 22.5 \mu\text{m}$; $\rho \approx 0.26$, $d \approx 6 \mu\text{m}$, $D \approx 23 \mu\text{m}$; $\rho \approx 0.16$, $d \approx 3 \mu\text{m}$, $D \approx 18 \mu\text{m}$	35×10^{-6}
$\text{Co}_{67}\text{Fe}_{3.85}\text{Ni}_{1.45}\text{B}_{11.5}\text{Si}_{14.5}\text{Mo}_{1.7}$	7A	$\rho \approx 0.16$, $d \approx 21.4 \mu\text{m}$, $D \approx 26.2 \mu\text{m}$	$< 10^{-7}$

^aEstimated from the data on amorphous wires in [12].

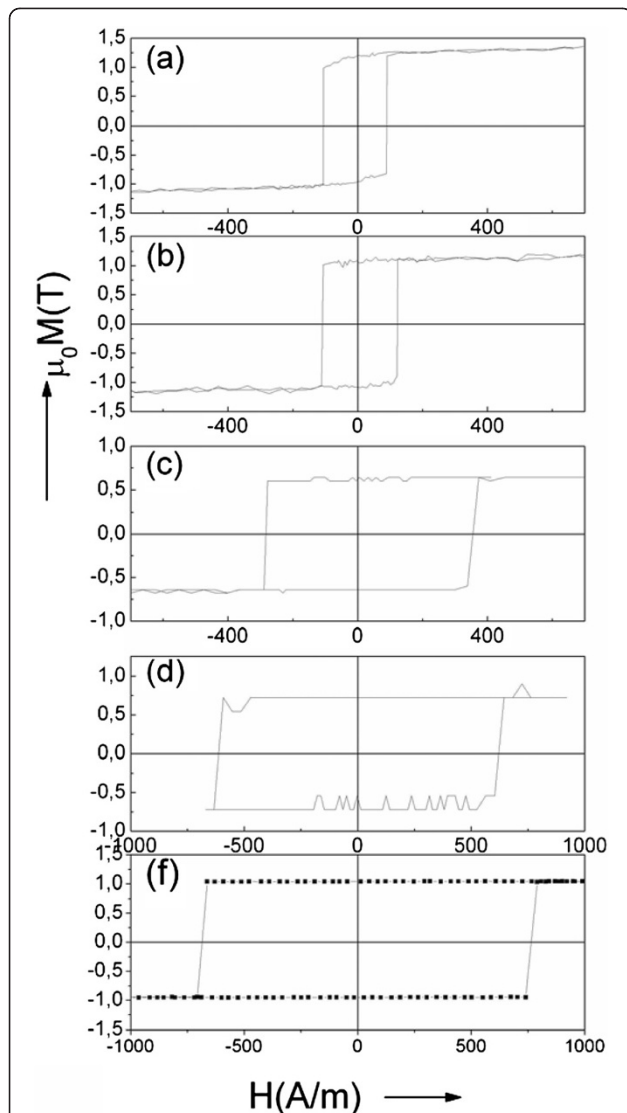


Figure 1 Hysteresis loops of Fe-rich amorphous microwires. All the samples have the same length and different metallic nucleus diameter d and total diameters D : Fe₇₀B₁₅Si₁₀C₅ microwires with $\rho = 0.63$, $d = 15 \mu\text{m}$ (a); $\mu = 0.48$, $d = 10.8 \mu\text{m}$ (b); $\mu = 0.26$, $d = 6 \mu\text{m}$ (c); $\mu = 0.16$, $d = 3 \mu\text{m}$ (d); and of Fe_{72.75}Co_{2.25}B₁₅Si₁₀ microwire with $\mu = 0.14$, $d \approx 1.4 \mu\text{m}$, $D \approx 10 \mu\text{m}$ (e).

In contrary to the classical Sixtus-Tonks experiments [16], we do not need the nucleation coils to nucleate the DW since the closure domain wall already exists. The small closure domains are created at the ends of the wire in order to decrease the stray fields [8]. Regarding experimental set-up, in order to activate DW propagation always from the other wire end in our experiment, we placed one end of the sample outside the magnetization solenoid. The microwire is placed coaxially inside of the primary and pick-up coils so that one end is inside of the primary coil. Magnetic field, H , is generated by solenoid applying rectangular-shaped voltage. The stresses have been applied

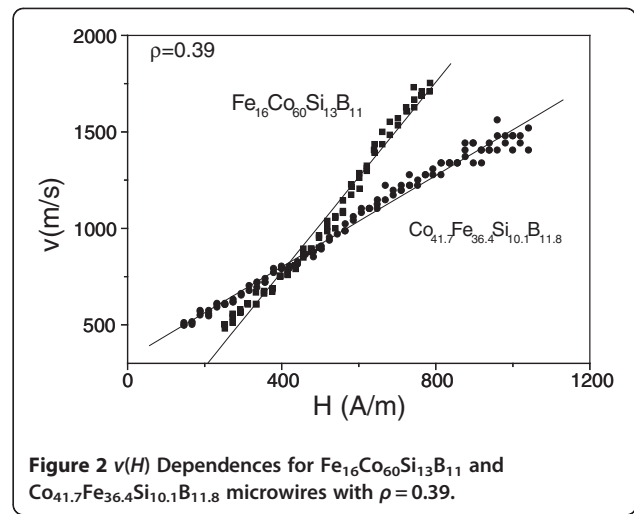


Figure 2 $v(H)$ Dependences for Fe₁₆Co₆₀Si₁₃B₁₁ and Co_{41.7}Fe_{36.4}Si_{10.1}B_{11.8} microwires with $\rho = 0.39$.

during DW dynamic measurements. We used three pick-up coils mounted along the length of the wire, and propagating DW induces electromotive force (emf) in the coils as described in [13]. These emf sharp peaks are picked up at an oscilloscope upon passing the propagating wall.

Then, DW velocity is estimated as:

$$v = \frac{l}{\Delta t} \quad (2)$$

where l is the distance between pick-up coils and Δt is the time difference between the maximum in the induced emf.

In our studies, we paid attention only to linear region of $v(H)$ corresponding to viscous DW propagation, leaving apart non-linearity at high-field region, attributed by different authors to Walker-like behavior [4,17] or multiple DW nucleation at defects [13]. Hysteresis loops have been measured using vibrating sample magnetometer.

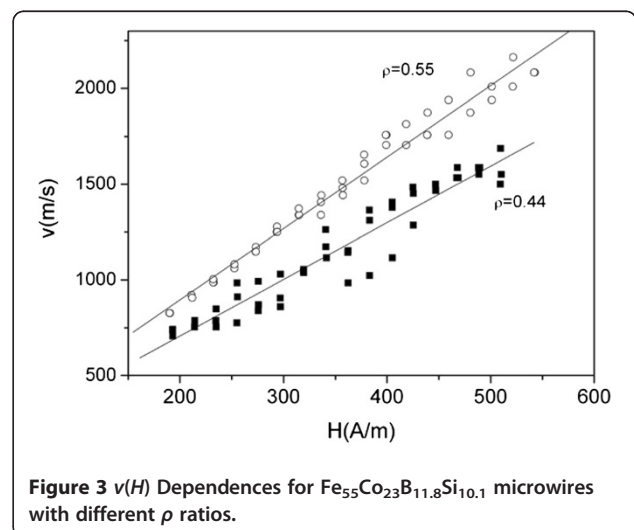
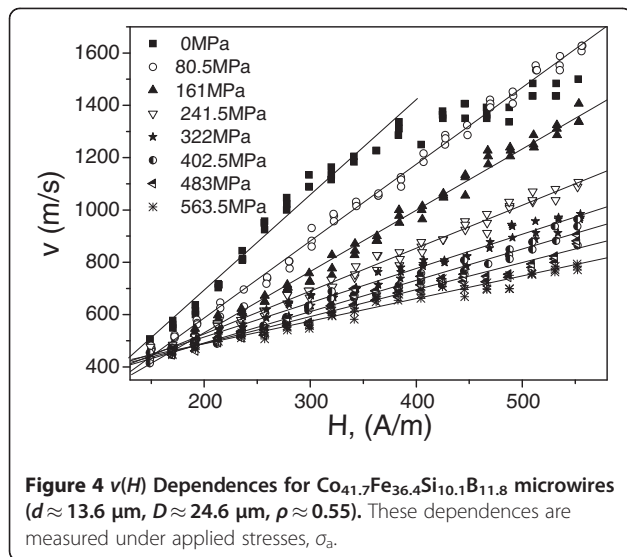
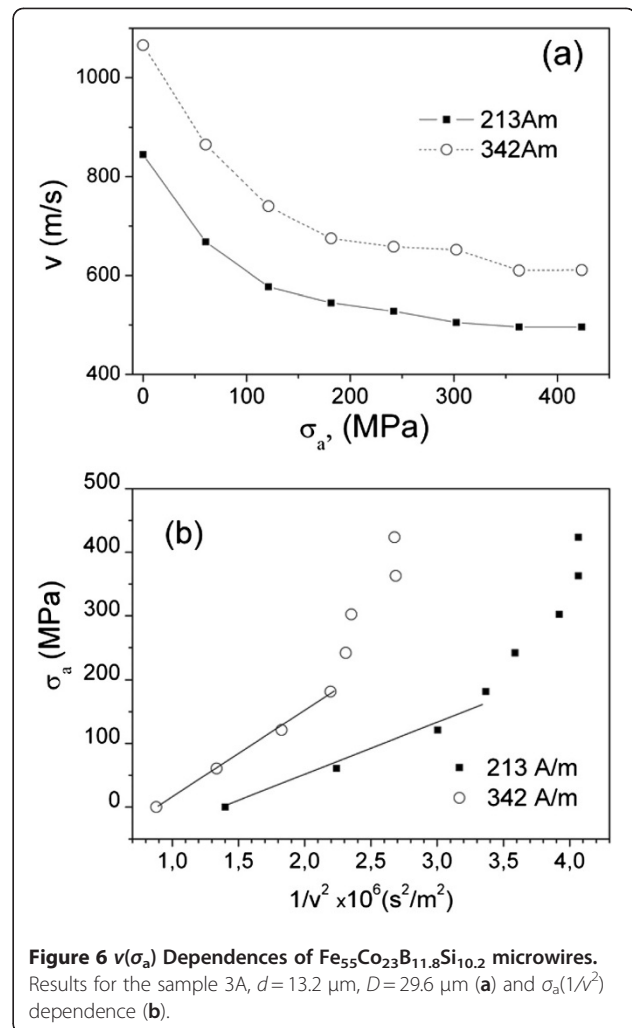
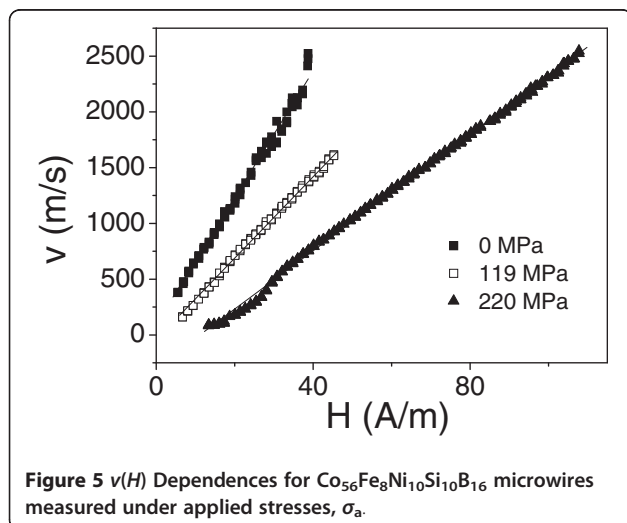


Figure 3 $v(H)$ Dependences for Fe₅₅Co₂₃B_{11.8}Si_{10.1} microwires with different ρ ratios.



Results and discussion

Hysteresis loops of a few studied microwires ($\text{Fe}_{70}\text{B}_{15}\text{Si}_{10}\text{C}_5$ and $\text{Fe}_{72.75}\text{Co}_{2.25}\text{B}_{15}\text{Si}_{10}$) with different metallic nucleus diameters and similar Fe-rich composition are shown in Figure 1. As can be appreciated, considerable increase of the switching field (from about 80 to 700 A/m) is observed when ferromagnetic metallic nucleus diameter decreases from 15 to 1.4 μm (i.e., one order). At the same time, rectangular hysteresis loop shape is maintained even for the smallest microwire diameters. Previously, similar increasing of coercivity with decreasing the metallic nucleus diameters has been attributed to enhanced magnetoelastic energy arising from enhanced internal stresses when ρ ratio is small [5,8,14]. Consequently, one of the relevant parameters affecting strength of internal stresses and the magnetoelastic energy is ρ ratio.

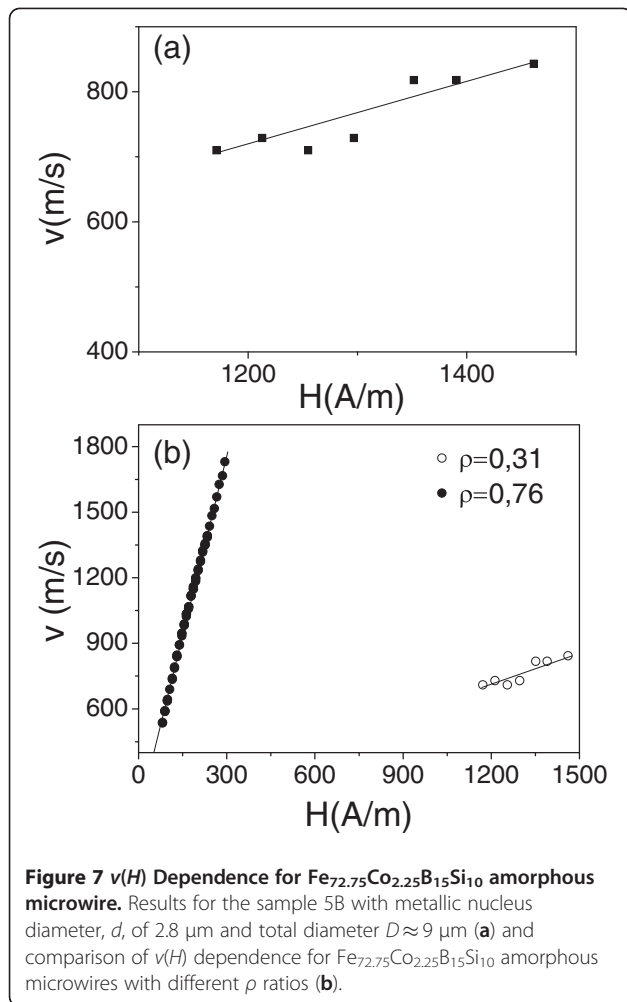


Usually, it is assumed that domain wall propagates along the wire with a velocity:

$$v = S(H - H_0) \quad (3)$$

where S is the DW mobility, H is the axial magnetic field, H_0 for $\text{Fe}_{16}\text{Co}_{60}\text{Si}_{13}\text{B}_{11}$ and $\text{Co}_{41.7}\text{Fe}_{36.4}\text{Si}_{10.1}\text{B}_{11.8}$ amorphous microwires with the same ρ ratio are shown in Figure 2. In this case, the effect of only magnetostriction constant is that higher magnetostriction constant (according to [12] for $\text{Co}_{41.7}\text{Fe}_{36.4}\text{Si}_{10.1}\text{B}_{11}$ microwire $\lambda_s \approx 25 \times 10^{-6}$ should be considered, while for $\text{Fe}_{16}\text{Co}_{60}\text{Si}_{13}\text{B}_{11}$ composition $\lambda_s \approx 15 \times 10^{-6}$, see Table 1) results in smaller DW velocity at the same magnetic field and smaller DW mobility, S .

In order to evaluate the effect of ρ ratio, i.e., effect of residual stresses on DW dynamics, we performed measurements of $v(H)$ dependences in the microwires with the same composition but with different ρ ratios. Dependences of DW velocity on the applied field for $\text{Fe}_{55}\text{Co}_{23}\text{B}_{11.8}\text{Si}_{10.1}$ microwires with different ratios are



shown in Figure 3. Like in Figure 2, at the same values of applied field, H , the domain wall velocity is higher for microwires with higher ρ ratio, i.e., when the internal stresses are lower [5,18].

The most efficient way to change *in situ* the magnetoelastic energy is to apply stresses during measurements. Therefore, to evaluate the magnetoelastic contribution, we measured $v(H)$ dependences applying stress. In this case, stress applied to metallic nucleus has been evaluated considering stresses distribution between the metallic nucleus and in glass coating, as previously described in [19]. We measured $v(H)$ dependences for various microwires with different magnetostriction constant, i.e., $\text{Co}_{41.7}\text{Fe}_{36.4}\text{Si}_{10.1}\text{B}_{11.8}$ microwire ($\rho \approx 0.55$) and $\text{Fe}_{74}\text{B}_{13}\text{Si}_{11}\text{C}_2$ microwire ($\rho \approx 0.67$) under applied stresses (see Figure 4 where $v(H)$ for microwire $\text{Co}_{41.7}\text{Fe}_{36.4}\text{Si}_{10.1}\text{B}_{11.8}$ is shown). Considerable decreasing of domain wall velocity, v , at the same magnetic field value, H , has been observed under applied stress. Additionally, increasing of applied stress, σ_a , results in decreasing of DW velocity.

Finally, we measured $v(H)$ dependences in low magnetostrictive $\text{Co}_{56}\text{Fe}_8\text{Ni}_{10}\text{Si}_{10}\text{B}_{16}$ microwire. DW velocity values achieved in this microwire (see Figure 5) at the same values of applied field are considerably higher (almost twice) than those observed for microwires with higher magnetostriction constant (see Figures 2, 3, and 4).

Regarding experimentally obtained $v(H)$ dependences shown in Figures 2, 3, 4, and 5, there are few typical features already discussed in previous publications. Thus, linear extrapolation to zero domain wall velocity (see Figures 2 and 5) gives negative values of the critical propagation field, H_0 . Such a negative value, previously reported for instance in [17,20], has been explained in terms of the negative nucleation field of the reversed domain. In the case of amorphous microwires, the reversed domain already exists and does not need to be nucleated by the reversed applied magnetic field. Another typical feature is non-linearity of $v(H)$ dependences at low-field region. Such deviations from linear dependence have been previously attributed to the domain wall interaction with the distributed defects [17,20].

The domain wall dynamics in viscous regime is determined by a mobility relation (Equation 3), where S is the domain wall mobility given by:

$$S = 2\mu_0 M_s / \beta \quad (4)$$

where β is the viscous damping coefficient and μ_0 is the magnetic permeability of vacuum. Damping is the most relevant parameter determining the domain wall dynamics. Various contributions to viscous damping β have been considered, and two of them are generally accepted [4,20-22]: micro-eddy currents circulating nearby moving domain wall are the more obvious cause of damping in metals. However, the eddy current parameter β_e is considered to be negligible in high-resistive materials, like thin amorphous microwires.

The second generally accepted contribution of energy dissipation is magnetic relaxation damping, β_r , related to a delayed rotation of electron spins. This damping is related to the Gilbert damping parameter and is inversely proportional to the domain wall width δ_w [20-22],

$$\beta_r \approx \alpha M_s / \gamma \Delta \approx M_s (K_{me} / A)^{1/2} \quad (5)$$

where γ is the gyromagnetic ratio, A is the exchange stiffness constant, and K_{me} is the magnetoelastic anisotropy energy given by Equation 1.

Consequently, we can assume that the magnetoelastic energy can affect domain wall mobility, S , as we experimentally observed in few Co-Fe-rich microwires. Additionally, as previously shown in [23], the magnetic relaxation damping, β_r , gives the main contribution to the total damping, β ,

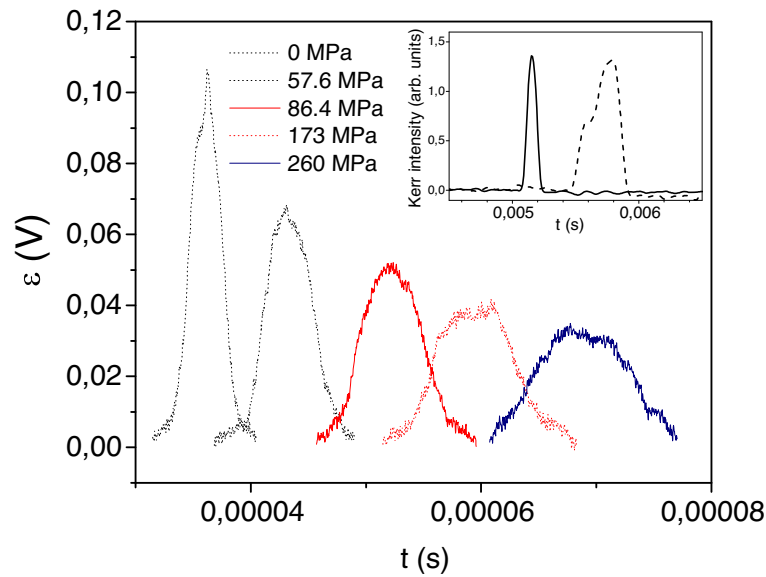


Figure 8 Change of shape of the voltage from pick-up coil under tensile stress application. Results for the sample 6A ($\text{Fe}_{70}\text{B}_{15}\text{Si}_{10}\text{C}_5$, $d \approx 14.6 \mu\text{m}$, $D \approx 21.8 \mu\text{m}$, $\mu \approx 0.67$). Inset, DC axial magnetic field induced transformation of the shape of the MOKE jump derivative: solid line, $H_{\text{ax}} = 0$; dashed line, $H_{\text{ax}} = 10 \text{ A/m}$.

when the wires are in stressed state, as the case of glass-coated microwires where glass coating induces strong internal stresses inside the metallic nucleus.

It is worth mentioning that systematic analysis of mechanisms of DW dynamics in thicker (with diameters between 30 and 120 μm) magnetostrictive amorphous wires without glass has been performed in [22] on the basis of bubble domain dynamics. The systematic analysis method in this paper is also a strong basis for considering domain propagation dynamics in glass-covered thinner magnetostrictive amorphous wires. Main assumptions on domain wall configuration in thicker wires have been performed considering that the DW length, l , is much more than its radius, r ($r/l < 10^{-3}$). Consequently recently, we tried to extend the analysis performed in [22] to thinner glass-coated microwires (typically with diameters 10 μm) with strong internal stresses induced by the glass coating [24]. Particularly analyzing the voltage peak forms and experimental data on DW dynamics, we demonstrated that a very high DW mobility observed in magnetically bistable amorphous microwires with a diameter of about 10 μm can be associated with elongated domain shape. The experimental results can be explained in terms of the normal mobility with respect to the domain surface, which is reduced by a factor representing the domain aspect ratio estimated to be 300 for considered wire samples. On the other hand, experimental data on DW dynamics in thin microwires and analysis of the voltages on pick-up coils show that, generally, the structure of propagating DW is far from abrupt and quite complex [9,25]. Thus, the

characteristic width of the head-to-head DW, δ , depends on many factors such as applied magnetic field, H : at $H = 60 \text{ A/m}$, $\delta \approx 65 \text{ d}$, while at $H = 300 \text{ A/m}$, $\delta \approx 40 \text{ d}$. Additionally, δ depends on magnetic anisotropy constant, K , being $\delta/d \approx 13.5$ for $K = 10^4 \text{ erg/cm}^3$, $\delta/d \approx 20$ for $K = 5 \times 10^3 \text{ erg/cm}^3$, $\delta/d = 30$ to 34 for $K = 2 \times 10^3 \text{ erg/cm}^3$, and $\delta/d = 40$ to 50 for $K = 10^3 \text{ erg/cm}^3$, respectively [25].

The numerical simulation of the head-to-head domain wall structure in nanowires with diameter d approximately 10 to 40 nm [26] shows that the characteristic DW width is comparable with the wire diameter, δ/d approximately 1 to 2. This is because the exchange energy contribution to the total nanowire energy dominates at very small diameters. However, with increasing of the wire diameter, the relative value of the exchange energy contribution decreases. However, for thinner wires with strong magnetoelastic anisotropy, the conditions $r/l < 10^{-3}$ considered in [22] are not realized.

On the other hand, from the aforementioned, we can consider that stress dependence of DW velocity, v , should exhibit an inverse square root dependence. In Figures 6, we present our attempt to evaluate quantitatively observed $v(\sigma_a)$ dependence for $\text{Fe}_{55}\text{Co}_{23}\text{B}_{11.8}\text{Si}_{10.2}$ microwires ($d = 13.2 \mu\text{m}$, $D = 29.6 \mu\text{m}$). Experimental $v(\sigma_a)$ dependence exhibits decreasing of DW velocity, v , with applied stresses, σ_a , (Figure 6a), but this dependence does not fit well with inverse square root dependence on the applied stress (Figure 6b). Here, we plotted the obtained experimentally dependences as $\sigma_a (v^{-2})$. From Figure 6b, we can conclude that the obtained $v(\sigma_a)$

dependences cannot be described by single $v(\sigma_a^{-1/2})$ dependence. One of the possible reasons of such deviation from the predicted dependence is that when applied stresses are of the same order, as the internal stresses with complex tensor character, the effect of applied stresses on DW dynamics cannot be considered in so simple assumption. It is worth mentioning that strong internal stresses may affect magnetic properties (particularly magnetic anisotropy) of such composite materials by quite unusual way [23]. The other reason can be related with stress dependence of magnetostriction previously observed in various amorphous alloys [27]. Additionally, applied stress affects electrical resistance and, consequently, can also affect the eddy current parameter β_e [28].

Regarding the aforementioned, it is interesting to compare the velocity of DW propagation in the thinnest microwire with the values observed in submicrometric planar nanowires reported elsewhere [29]. The DW velocity in thin microwire is ranging between 700 and 850 m/s (Figure 7a), which is still higher than for the same range of magnetic field as compared with submicrometric nanowires (maximum $v \approx 110$ m/s at 700 A/m) reported elsewhere [29].

Indeed, at least in $\text{Fe}_{72.75}\text{Co}_{2.25}\text{B}_{15}\text{Si}_{10}$ amorphous microwire with a metallic nucleus diameter of 2.8 μm , we were able to observe domain wall propagation by the above described (Sixtus-Tonks-like) method. For such elevated magnetic fields (13 to 20 Oe), the domain wall velocity, v , is significantly lower than for thicker wires. For comparison, $v(H)$ dependence for $\text{Fe}_{74}\text{Si}_{11}\text{B}_{13}\text{C}_2$ microwire with similar composition with metallic nucleus d and total D diameters 12.0/15.8 is presented in Figure 7b. As can be deduced from comparison of DW dynamics, thicker $\text{Fe}_{74}\text{Si}_{11}\text{B}_{13}\text{C}_2$ microwire at maximum achieved magnetic field (about 280 A/m) presented double higher velocity as compared with $\text{Fe}_{72.75}\text{Co}_{2.25}\text{B}_{15}\text{Si}_{10}$ amorphous microwire with metallic nucleus diameter, d , of 2.8 μm and total diameter $D \approx 9$ μm (Figure 7b).

Regarding the observed differences on $v(H)$ dependences, one should consider enhanced magnetoelastic energy for $\text{Fe}_{72.75}\text{Co}_{2.25}\text{B}_{15}\text{Si}_{10}$ amorphous microwire since ratio $\rho = d/D$ determining strength of internal stresses [14,15] for thin $\text{Fe}_{72.75}\text{Co}_{2.25}\text{B}_{15}\text{Si}_{10}$ is $\rho \approx 0.31$, while for thicker $\text{Fe}_{74}\text{Si}_{11}\text{B}_{13}\text{C}_2$ microwire, $\rho \approx 0.56$.

This also reflected by the change of the shape of the voltage induced in the pick-up coil surrounding microwires under tensile stress application (see Figure 8 for the $\text{Fe}_{74}\text{B}_{13}\text{Si}_{11}\text{C}_2$ microwire with $\lambda_s \approx 35 \times 10^{-6}$). As-prepared microwires exhibit quite sharp voltage peaks induced in the pick-up coil associated with fast magnetization switching with the half width of the peak about 3 μs . Applying tensile stress, the half width

gradually increases and at 260 MPa achieves about 8 μs . Such increasing of the half width reflects decreasing of DW velocity under tensile stress application.

Additionally, the decreasing of the DW velocity related to DW transformation has been observed when the magneto-optical Kerr effect (MOKE) modified Sixtus-Tonks method [30] has been used (see inset in Figure 8 for $\text{Co}_{67}\text{Fe}_{3.85}\text{Ni}_{1.45}\text{B}_{11.5}\text{Si}_{14.5}\text{Mo}_{1.7}$ microwire, metallic nucleus radius 10.7 μm , glass coating thickness 2.4 μm with $\lambda_s \approx 10^{-7}$). Application of DC axial magnetic field (H_{ax}) additionally to the driving pulsed circular magnetic field causes the considerable transformation of the MOKE peak that in turn finds the reflection in DW deceleration. In the latter case, sharper voltage peaks, as compared with Fe-rich microwire, reflect higher DW velocity which should be attributed to lower magnetostriction constant of the Co-rich microwire.

Conclusions

In summary, we experimentally observed that when manipulating the magnetoelastic energy through application of tensile stress and changing the magnetostriction constant and internal stresses of studied microwires, we significantly affected the domain wall dynamics in magnetically bistable microwires. Considering the aforementioned, we assume that in order to achieve higher DW propagation velocity at the same magnetic field and enhanced DW mobility, special attention should be paid to decreasing of magnetoelastic energy.

Competing interests

The authors declare that they have no competing interests.

Acknowledgments

This work was supported by the EU ERA-NET programme under project 'SoMaMicSens' (MANUNET-2010-Basque-3), by the Spanish MICINN under project MAT2010-18914, and by the Basque Government under Saiotek 10 MIMAGURA project.

Author details

¹Department of Material Physics, Chemistry Faculty, Universidad del País Vasco/Euskal Herriko Unibertsitatea (UPV/EHU), P.O. Box 1072, San Sebastián 20080, Spain. ²IKERBASQUE, Basque Foundation for Science, Bilbao 48011, Spain. ³Department of Applied Physics I, Escuela Universitaria Politécnica Donostia-San Sebastián (EUPDS), Universidad del País Vasco/Euskal Herriko Unibertsitatea (UPV/EHU), Plaza Europa 1, San Sebastián 20018, Spain.

Authors' contributions

AZ provided the samples and participated in the interpretation of results. JMB measured DW propagation. MI developed the experimental setup and measured DW propagation. AC measured DW propagation by magneto-optics. VZ provided the samples and participated in the interpretation of results. All authors read and approved the final manuscript.

Received: 16 January 2012 Accepted: 19 March 2012

Published: 18 April 2012

References

1. Allwood DA, Xiong G, Faulkner CC, Atkinson D, Petit D, Cowburn RP: Magnetic domain-wall logic. *Science* 2005, **309**:1688–1692.

2. Hayashi M, Thomas L, Rettner Ch, Moriya R, Jiang X, Parkin S: **Dependence of current and field driven depinning of domain walls on their structure and chirality in permalloy nanowires.** *Phys Rev Lett* 2006, **97**(4):207205.
3. Zhukov A: **Domain wall propagation in a Fe-rich glass-coated amorphous microwire.** *Appl Phys Lett* 2001, **78**:3106–3108.
4. Varga R, Zhukov A, Zhukova V, Blanco JM, Gonzalez J: **Supersonic domain wall in magnetic microwires.** *Phys Rev B* 2007, **76**(3):132406.
5. Chiriac H, Ovari TA, Pop Gh: **Internal stress distribution in glass-covered amorphous magnetic wires.** *Phys Rev B* 1995, **52**(14):10104–10113.
6. Vázquez M, García-Beneytez JM, García JM, Sinnecker JP, Zhukov A: **Giant magneto-impedance in heterogeneous microwires.** *J Appl Phys* 2000, **88**(11):6501–6505.
7. Zhukov AP: **The remagnetization process of bistable amorphous alloys.** *Mater Des* 1993, **5**:299.
8. Zhukov AP, Vázquez M, Velázquez J, Chiriac H, Larin V: **The remagnetization process of thin and ultrathin Fe-rich amorphous wires.** *J Magn Magn Mater* 1995, **151**:132.
9. Ekstrom PA, Zhukov A: **Spatial structure of the head-to-head propagating domain wall in glass-covered FeSiB microwire.** *J Phys D: Appl Phys* 2010, **43**:205001.
10. Antonov AS, Borisov VT, Borisov OV, Prokoshin AF, Usov NA: **Residual quenching stresses in glass-coated amorphous ferromagnetic microwires.** *J Phys D: Appl Phys* 2000, **33**:1161–1168.
11. Blanco JM, Zhukova V, Ipatov M, Zhukov A: **Effect of applied stresses on domain wall propagation in glass-coated amorphous microwires.** *Phys Status Solidi A* 2011, **208**(3):545–548.
12. Konno Y, Mohri K: **Magnetostriction measurements for amorphous wires.** *IEEE Trans Magn* 1989, **25**(5):3623–3625.
13. Ipatov M, Zhukova V, Zvezdin AK, Zhukov A: **Mechanisms of the ultrafast magnetization switching in bistable amorphous microwires.** *J Appl Phys* 2009, **106**(5):103902.
14. Zhukov A, Zhukova V: *Magnetic Properties and Applications of Ferromagnetic Microwires with Amorphous and Nanocrystalline Structure.* New York: Nova Science Publishers, Inc.; 2009.
15. Chiriac H, Óvári T-A, Corodeanu S, Ababei G: **Interdomain wall in amorphous glass-coated microwires.** *Phys. Rev B* 2007, **76**:214433.
16. Sixtus KJ, Tonks L: **Propagation of large Barkhausen discontinuities.** *Phys Rev* 1932, **42**:419–435.
17. Varga R, Garcia KL, Vázquez M, Vojtanik P: **Single-domain wall propagation and damping mechanism during magnetic switching of bistable amorphous microwires.** *Phys Rev Lett* 2005, **94**(4):017201.
18. Chiriac H, Ovari T-A, Zhukov A: **Magnetoelastic anisotropy of amorphous microwires.** *J Magn Magn Mater* 2003, **254–255**:469–471.
19. Zhukov A: **Design of the magnetic properties of Fe-rich, glass-coated microwires for technical applications.** *Adv Func Mat* 2006, **16**:675–680.
20. Varga R, Richter K, Zhukov A, Larin V: **Domain wall propagation in thin magnetic wires.** *IEEE Trans Magn* 2009, **44**(11):3925–3932.
21. Infante G, Varga R, Badini-Confalonieri GA, Vázquez M: **Locally induced domain wall damping in a thin magnetic wire.** *Appl Phys Lett* 2009, **95**(3):012503.
22. Panina LV, Mizutani M, Mohri K, Humphrey FB, Ogasawara I: **Dynamics and relaxation of large Barkhausen discontinuity in amorphous wires.** *IEEE Trans Magn* 1991, **27**(6):5331–5333.
23. Zhukova V, Larin VS, Zhukov A: **Stress induced magnetic anisotropy and giant magnetoimpedance in Fe-rich glass-coated magnetic microwires.** *J Appl Phys* 2003, **94**(2):1115–1118.
24. Panina LV, Ipatov M, Zhukova V, Zhukov A: **Domain wall propagation in Fe-rich amorphous microwires.** *Physica B* 2012. doi:10.1016/j.physb.2011.06.047.
25. Gudoshnikov SA, Grebenshchikov Yu B, Ya Ljubimov B, Palvanov PS, Usov NA, Ipatov M, Zhukov A, Gonzalez J: **Ground state magnetization distribution and characteristic width of head to head domain wall in Fe-rich amorphous microwire.** *Phys Status Solidi A* 2009, **206**(4):613–617.
26. Usov NA, Zhukov A, Gonzalez J: **Domain walls and magnetization reversal process in soft magnetic nanowires and nanotubes.** *J Magn Magn Mater* 2007, **316**:255–261.
27. Aragonese P, Blanco JM, Dominguez L, González J, Zhukov A, Vázquez M: **The stress dependence of the switching field in glass-coated amorphous microwires.** *J Phys D: Appl Phys* 1998, **31**:3040–3045.
28. Blodgett MP, Nagy PB: **Eddy current assessment of near-surface residual stress in shot-peened nickel-base superalloys.** *J Nondestructive Eval* 2004, **23**:107–123.
29. Beach GSD, Tsoi M, Erskine JL: **Current-induced domain wall motion.** *J Magn Magn Mater* 2008, **320**:1272–1281.
30. Chizhik A, Varga R, Zhukov A, Gonzalez J, Blanco JM: **Kerr-effect based Sixtus-Tonks experiment for measuring the single domain wall dynamics.** *J Appl Phys* 2008, **103**(3):07E707.

doi:10.1186/1556-276X-7-223

Cite this article as: Zhukov et al.: Manipulation of domain wall dynamics in amorphous microwires through the magnetoelastic anisotropy. *Nanoscale Research Letters* 2012 **7**:223.

Submit your manuscript to a SpringerOpen[®] journal and benefit from:

- Convenient online submission
- Rigorous peer review
- Immediate publication on acceptance
- Open access: articles freely available online
- High visibility within the field
- Retaining the copyright to your article

Submit your next manuscript at ► springeropen.com